HHS Public Access

Author manuscript

Nat Struct Mol Biol. Author manuscript; available in PMC 2019 November 27.

Published in final edited form as:

Nat Struct Mol Biol. 2019 June ; 26(6): 450–459. doi:10.1038/s41594-019-0230-1.

CAT tails drive degradation of stalled polypeptides on and off the ribosome

Cole S. Sitron[1] and **Onn Brandman**[1,*]

[1]Department of Biochemistry, Stanford University, Stanford, CA, USA.

Abstract

Stalled translation produces incomplete, ribosome-tethered polypeptides that the Ribosome-associated Quality Control (RQC) pathway targets for degradation via the E3 ubiquitin ligase Ltn1. During this process, the protein Rqc2 and the large ribosomal subunit elongate stalled polypeptides with carboxy-terminal alanine and threonine residues (CAT tails). Failure to degrade CAT-tailed proteins disrupts global protein homeostasis, as CAT-tailed proteins can aggregate and sequester chaperones. Why cells employ such a potentially toxic process during RQC is unclear. Here, we developed quantitative techniques to assess how CAT tails affect stalled polypeptide degradation in *Saccharomyces cerevisiae*. We found that CAT tails enhance Ltn1's efficiency in targeting structured polypeptides, which are otherwise poor Ltn1 substrates. If Ltn1 fails to ubiquitylate those stalled polypeptides or becomes limiting, CAT tails act as degrons, marking proteins for proteasomal degradation off the ribosome. Thus, CAT tails functionalize the carboxy-termini of stalled polypeptides to drive their degradation on and off the ribosome.

Introduction

Stalled mRNA translation produces incomplete polypeptides that can be deleterious to cells. In eukaryotes, the Ribosome-associated Quality Control (RQC) pathway recognizes these stalled polypeptides while they are attached to ribosomes and targets them for degradation[1–3]. RQC targets a variety of stalled polypeptides generated by diverse translation abnormalities, including truncated mRNA[4,5], inefficiently decoded codons[6], and translation past stop codons into poly(A) tails[1,7].When stalling occurs, the slowdown of translation causes adjacent ribosomes to collide. The interface between the stalled ribosomes forms a signal recognized by the E3 ubiquitin ligase Hel2 (ZNF598 in mammals)[8–10]. Hel2 then ubiquitylates 40S ribosomal proteins, triggering RQC[11–13]. After this process of stall

* onn@stanford.edu.

Author Contributions

O.B. and C.S.S. conceived of the study and designed the experiments. C.S.S. performed the experiments. O.B. and C.S.S. analyzed and interpreted the data. O.B. and C.S.S. wrote the manuscript. O.B. supervised the study.

Competing Interests

The authors declare no competing interests.

Data Availability

The datasets that inform the conclusions of this study are available from the corresponding author upon request.

recognition occurs, RQC factors remodel the ribosome to produce a 60S subunit-stalled polypeptide complex[4,5,11–17].

Studies on RQC mechanism have focused on the 60S subunit-stalled polypeptide complex as the sole opportunity for the cell to target stalled polypeptides (RQC substrates) for degradation. Two proteins, Ltn1 and Rqc2, bind that complex and play central roles in degrading the stalled polypeptide[1–3,5,16]. Ltn1, a RING E3 ubiquitin ligase, ubiquitylates the RQC substrate while it is tethered to the 60S ribosome to mark it for proteasome-mediated degradation[1–3,5]. Rqc2 facilitates Ltn1 binding to the ribosome and drives the C-terminal addition of alanine and threonine ("CAT tails", "CATylation") to the RQC substrate[3,18–20]. Unlike conventional translation, CATylation occurs without an mRNA template or the 40S ribosomal subunit[19,20]. Failure to degrade CATylated proteins can result in their aggregation and lead to disruption of global protein homeostasis in yeast[21–23]. Intriguingly, mutation of Ltn1, which is the only E3 ligase known to ubiquitylate CATylated proteins, leads to progressive neurodegeneration in mice[24]. Given the inherent risk associated with generating aggregation-prone polypeptides, the evolution and function of CATylation are subjects of intense interest.

As a consequence of CAT tail extension, amino acid residues previously buried in the ribosome become exposed to the environment outside of the ribosome exit tunnel. Kostova and colleagues proposed that the ~12 amino acids of the RQC substrate emerging from the exit tunnel are the only residues that Ltn1 can efficiently ubiquitylate[25]. If a substrate lacks lysine residues within this window, the authors propose that CAT tail extension extrudes any lysine residues buried in the exit tunnel, exposing them for Ltn1 to ubiquitylate[25]. This model suggests that Ltn1 activity is limited by RQC substrate primary structure and that CAT tails aid degradation of RQC substrates by expanding the region of Ltn1-accessible residues to include those within the ribosome exit tunnel.

In this work, we assessed the contribution of CAT tails to degradation of model RQC substrates using new, quantitative approaches. We found that CATylation enhances degradation of RQC substrates both on and off the ribosome. On the ribosome, CATylation enhances Ltn1's ability to ubiquitylate structured substrates, which Ltn1 otherwise targets inefficiently. Contrary to the model proposed by Kostova et al.[25], our data indicate that Ltn1 is not restricted to lysine residues proximal (in primary structure) to the exit tunnel and that CAT tails can enable Ltn1 to access residues other than those in the exit tunnel. Moreover, we found that CAT tails provide cells with an additional opportunity to degrade RQC substrates that escape ubiquitylation on the 60S ribosome. Off the ribosome, CAT tails act as degrons to mark those escaped RQC substrates for proteasomal degradation, independently of Ltn1. For the substrates we analyzed, Ltn1-independent degradation required the E3 ubiquitin ligase Hul5.

Results

CAT tails aid decay of RQC substrates

To measure how CAT tails contribute to RQC substrate degradation, we monitored how disruption of CATylation affects steady-state levels of model RQC substrates in

Saccharomyces cerevisiae. Each model substrate contained an N-terminal green fluorescent protein (GFP) followed by a flexible linker, tobacco etch virus (TEV) protease cleavage site, and stall-inducing polyarginine sequence (Fig. 1b,c). Ribosomes begin translating these substrates normally but stall within the polyarginine sequence without reaching the stop codon[26]. This produces a GFP-linker-arginine nascent polypeptide that is a substrate for RQC[2].

We began by constructing two model RQC substrates that differed in the length of the linker ($RQCsub_{SHORT}$, $RQCsub_{LONG}$), allowing two variants for how much of the GFP-linker-arginine polypeptide protruded from the ribosome exit tunnel (Fig. 1b,c). *ltn1*Δ strains accumulated more $RQCsub_{SHORT}$ and $RQCsub_{LONG}$ protein products by SDS-PAGE than *LTN1-WT* strains, confirming that both are substrates for Ltn1 and, thus, RQC (Fig. 1b,c). $RQCsub_{SHORT}$ and $RQCsub_{LONG}$ protein products migrated as higher molecular weight smears in the *ltn1*Δ background when Rqc2 was intact (Fig. 1b,c). These smears collapsed onto discrete bands upon mutation of Rqc2 to the CATylation-incompetent *rqc2-d98a* mutant[19] or cleavage of the C-terminus by TEV protease treatment (Fig. 1b,c), indicating that the smears contained CAT tails of varying length. Strikingly, loss of CATylation with *rqc2-d98a* led to an accumulation of $RQCsub_{LONG}$ but not $RQCsub_{SHORT}$ (Fig. 1b,c). These qualitative results suggest that CAT tails enable efficient degradation of some RQC substrates but not others.

To explore the differences in degradation between $RQCsub_{SHORT}$ and $RQCsub_{LONG}$, we developed a quantitative assay to measure the extent to which RQC substrate degradation depends on CAT tails. We constructed an internal expression control by adding red fluorescent protein (RFP) followed by tandem viral T2A skipping peptides upstream of GFP-linker arginine (Fig. 1d). During each round of translation, the ribosome skips formation of a peptide bond within the T2A sequence, producing an RFP that detaches from GFP-linker-arginine before stalling occurs[27,28]. This detachment ensures that RQC targets GFP-linker-arginine but not RFP. Indeed, *ltn1*Δ did not increase RFP levels compared to wild-type (Supplementary Fig. 1a), confirming that RFP is not an RQC substrate. Because the ribosome synthesizes the two fluorescent proteins stoichiometrically but RQC only targets GFP, the GFP:RFP ratio reports on RQC substrate stability. By comparing stability between an experimental condition and a condition where CATylation and RQC are inactive (*rqc2-d98a ltn1*Δ), we controlled for any RQC-independent degradation or change in fluorescence. This strategy eliminated noise inherent in our model RQC substrate expression system (Supplementary Fig. 1b) and allowed us to quantitatively compare different RQC substrates.

Using our quantitative assay, we re-assessed how degradation of $RQCsub_{SHORT}$ and $RQCsub_{LONG}$ depends on CAT tails. We defined “CAT tail dependence” as the change in protein stability due to CATylation impairment, i.e. $\text{stability}_{rqc2\text{-}d98a} - \text{stability}_{RQC2\text{-}WT}$ (Fig. 1d). Consistent with our previous qualitative results (Fig. 1b,c), CAT tail dependences for $RQCsub_{LONG}$ and $RQCsub_{SHORT}$ were 24% and 0.8%, respectively (Fig. 1e). Additionally, we observed substantial CAT tail dependence independent of Ltn1 (in the *ltn1*Δ background) (Supplementary Fig. 1c and below). To ensure that the CAT tail dependence observed for $RQCsub_{LONG}$ was not an artifact of changes in ribosome stalling, we designed a quantitative

stalling reporter similar to one used by the Hegde and Bennett groups[9,11,12]: *RQC2* or *LTN1* mutations did not affect stalling relative to control (Supplementary Fig. 1d). Furthermore, expressing RQCsub$_{LONG}$ using the strong *TDH3* promoter and the moderate *MET17* promoter yielded identical stabilities (Supplementary Fig. 1e), suggesting that CAT tail dependence did not require RQCsub$_{LONG}$ overproduction. These data suggest that CAT tails facilitate degradation of RQCsub$_{LONG}$ but are dispensable for RQCsub$_{SHORT}$.

A previous study proposed that CAT tails aid degradation by extending the RQC substrate so that lysine residues buried in the ribosome exit tunnel emerge from the ribosome and can be ubiquitylated by Ltn1[25]. RQCsub$_{LONG}$ has its most C-terminal lysine residue 24 amino acids away from the stall sequence, placing it in the 35–40 amino-acid-long exit tunnel[29] at the point of stalling. However, mutation of this single buried lysine to arginine (which cannot be ubiquitylated) preserved the bulk of CAT tail dependence (from 24% to 19%) (Fig. 1f; Supplementary Fig. 1f). Similarly, mutation of ten lysine residues in the C-terminal half of RQCsub$_{LONG}$ maintained CAT tail dependence (from 24% to 22%) (Fig. 1f). Although these mutations placed the proximal lysine 150 residues from the stall sequence, *ltn1*Δ still stabilized this substrate (Supplementary Fig. 1f). These data suggest that Ltn1 activity is not restricted to lysine residues close (in primary structure) to the exit tunnel. Therefore, CAT tails can mediate degradation of RQC substrates without displacing lysine from the exit tunnel.

Substrate structure affects degradation

We next sought to find the properties of RQCsub$_{SHORT}$ and RQCsub$_{LONG}$ that drive their differences in CAT tail dependence. These substrates differ in their capacity to cotranslationally fold (Fig. 2a). After stalling occurs, the linker in RQCsub$_{LONG}$ is long enough to displace ten of the eleven GFP beta strands out of the exit tunnel, which enables the nascent GFP to adopt a stable conformation[30]. By contrast, the linker in RQCsub$_{SHORT}$ can only displace nine beta strands, preventing the formation of this stable conformation[30]. Thus, a difference in folding states between RQCsub$_{SHORT}$ and RQCsub$_{LONG}$ may account for their different CAT tail dependence.

To evaluate the hypothesis that CAT tails promote degradation of structured RQC substrates, we tested how modulating folding of the substrate changes CAT tail dependence. To modulate folding of RQCsub$_{LONG}$, we took advantage of the temperature-sensitive folding of the GFP variant (GFP-S65T) used in the substrate[31]. As incubation temperature increased (decreasing GFP-S65T folding capacity[31]), CAT tail dependence for RQCsub$_{LONG}$ decreased (Fig. 2b). When we replaced GFP-S65T with the less temperature-sensitive superfolder-GFP[31,32], RQCsub$_{LONG\text{-}superfolder}$ had high CAT tail dependence even at high temperatures (Fig. 2b). These data support a model where CAT tails enhance degradation of structured substrates but are dispensable for unstructured substrates.

To generalize our results beyond GFP, we next tested this hypothesis on spectrin, a protein whose co-translational folding is well-understood and easily modulated[33,34]. We designed RQCsub$_{SPECTRIN}$ using the same RFP-T2A module followed by a spectrin domain, a C-terminal GFP beta strand (β11), and lastly a polyarginine stall sequence. We quantified RQCsub$_{SPECTRIN}$ levels using a “split-GFP” strategy, co-expressing the N-terminal GFP

fragment from another transcript[35]. We observed that RQCsub$_{SPECTRIN}$ was 12% CAT tail dependent, while the folding-disrupting F11D mutation[33,34] eliminated CAT tail dependence (Fig. 2c; Supplementary Fig. 2a). These data suggest that the role of CAT tails in promoting degradation of structured RQC substrates is general, and not unique to GFP.

If CAT tails mediate degradation of structured RQC substrates, we would expect that addition of unfolded domains to a structured substrate would relax its CAT tail dependence for degradation. To test this hypothesis, we appended spectrin variants to the N-terminus of RQCsub$_{LONG}$. Folding-disrupted spectrin eliminated CAT tail dependence (from 24% to 1.7%) while folding-competent spectrin did not (from 24% to 28%) (Fig. 2d; Supplementary Fig. 2b). This finding prompted us to inquire whether the presence of unfolded domains alone or, instead, flexible lysine residues within the domains abrogate CAT tail dependence. To distinguish between these possibilities, we added unstructured FLAG-tag variants (with or without lysine residues) to the N-terminus of RQCsub$_{LONG}$. The lysine-containing FLAG-tag decreased CAT tail dependence (from 24% to 4.9%), 3.8-fold more than did the lysine-free FLAG-tag (19%) (Fig. 2e; Supplementary Fig. 2c). We thus propose that CAT tails preferentially enhance degradation of RQC substrates lacking lysine in unfolded regions.

Ltn1-independent degradation

While impairing CATylation affected the stability of some RQC substrates differently when Ltn1 was intact, impairing CATylation in the *ltn1*Δ background dramatically increased the stability of every substrate we measured (Supplementary Figs. 1,2). This indicated that CAT tails destabilize proteins independently of Ltn1. To evaluate whether this destabilization was due to CAT tail-induced proteolysis, we perturbed two mechanisms of proteolysis. Treatment with the proteasome inhibitor bortezomib increased the stability of RQCsub$_{LONG}$ in *ltn1*Δ, but only when CATylation was intact (Fig. 3a). By contrast, disruption of vacuolar proteolysis with *pep4*Δ had no effect on the stability of RQCsub$_{LONG}$ in *ltn1*Δ (Supplementary Fig. 3a). These data suggest that CAT tails target proteins for proteasomal degradation by Ltn1-dependent and -independent mechanisms.

Either the process of CATylation or CAT tails themselves could serve as an Ltn1-independent degradation signal. To distinguish between these possibilities, we employed a strategy to remove a substrate's CAT tail *in vivo* without disrupting the process of CATylation. We co-expressed RQCsub$_{LONG}$ and TEV protease *in vivo* to cleave RQCsub$_{LONG}$'s C-terminus and remove its CAT tail. TEV co-expression increased RQCsub$_{LONG}$'s mobility on SDS-PAGE (Supplementary Fig. 3b), confirming TEV activity *in vivo*. RQCsub$_{LONG}$ was stabilized by TEV co-expression in cells with Rqc2 intact but not in cells incapable of CATylation (*rqc2-d98a*) (Fig. 3b). Taken together, these results indicate that CATylation destabilizes proteins, but removal of the CAT tail blocks this destabilization. We conclude that CAT tails themselves target RQC substrates for Ltn1-independent degradation.

We next searched a set of candidate genes from the ubiquitin-proteasome system to identify an E3 ligase that ubiquitylates CATylated proteins in the absence of Ltn1. Deletion of the proteasome-associated E3 ligase *HUL5*[36] stabilized RQCsub$_{LONG}$ in the *ltn1*Δ background

as much as removing CATylation (*rqc2-d98a*) (Supplementary Fig. 3c). Furthermore, during a cycloheximide chase, *hul5*Δ slowed decay of RQCsub$_{LONG}$ in the *ltn1*Δ background as much as impaired CATylation (Supplementary Fig. 3d). This indicates that CATylated proteins are continuously degraded when Ltn1 is limiting. For CATylated RQCsub$_{LONG}$, this Ltn1-independent degradation required Hul5. The stabilization we observed after loss of Hul5 was not due to perturbed CATylation, as RQCsub$_{LONG}$ had identical amino acid composition in *ltn1Δ* and *hul5Δ ltn1Δ* (Supplementary Fig. 3e). When Ltn1 was intact, *hul5*Δ significantly stabilized RQCsub$_{LONG}$ with *RQC2-WT* but not *rqc2-d98a* (Fig. 3c). These modest effects observed in *rqc2-d98a* were likely non-specific, as *hul5*Δ also weakly stabilized a non-stalling degradation sequence ("degron")[37] (Supplementary Fig. 3f). These results support a role for the E3 ligase Hul5 in Ltn1-independent degradation of a model CATylated protein.

Hul5 has E4 ligase activity, which extends existing ubiquitin conjugates to create poly-ubiquitin chains that boost proteasome processivity[36,38,39]. It is thus possible that we identified Hul5 because degradation of CATylated proteins requires extension of a mono-ubiquitin mark left by another E3 ligase. A hallmark of E4 ligase activity is stabilization of the mono-ubiquitylated substrate after loss of the ligase[40,41], resulting in an 11kDa shift (His-Myc-Ubiquitin) by SDS-PAGE. However, purification of RQCsub$_{LONG}$ in the *ltn1*Δ background revealed that *hul5*Δ, like *rqc2-d98a*, diminished detection of ubiquitylated conjugates without stabilizing an apparent mono-ubiquitylated species (Fig. 3d). Thus, Hul5 is required for an E3 ligase activity that ubiquitylates our model CATylated protein.

While *hul5*Δ did not stabilize a mono-ubiquitylated RQCsub$_{LONG}$ species in the *ltn1*Δ background, *hul5*Δ intensified a crisp band within the CATylated smear, ~1kDa above the lowest band (Fig. 3d; Supplementary Fig. 4a). This band disappeared after disruption of CATylation (*rqc2-d98a*) (Fig. 3d), suggesting that the corresponding protein contains short CAT tails of relatively uniform size (~10–14 residues). To test whether short CAT tails support Hul5-dependent degradation, we monitored RQCsub$_{LONG}$ stability in the presence of *rqc2-d9a*, an *RQC2* mutant that produces short CAT tails (Supplementary Fig. 4b). In the *ltn1*Δ background, *rqc2-d9a* preserved the majority of RQCsub$_{LONG}$ stabilization after *hul5*Δ that we observed for *RQC2-WT* (Supplementary Fig. 4c). We posit that short CAT tails mark proteins for destruction.

CAT tails can decrease the solubility of RQC substrates and drive the formation of aggregates[21–23]. We asked whether blocking Ltn1-independent degradation of CATylated RQCsub$_{LONG}$ potentiates its aggregation. As expected, blocking Ltn1-independent degradation of RQCsub$_{LONG}$ with *hul5*Δ led to greater accumulation of the substrate, as seen by SDS-PAGE in *hul5*Δ *ltn1*Δ lysates relative to *ltn1*Δ lysates (Supplementary Fig. 4d, "input" fractions). Fractionation of *ltn1*Δ lysates containing RQCsub$_{LONG}$ revealed that disruption of Ltn1-independent degradation with *hul5*Δ slightly increased RQCsub$_{LONG}$ deposition into the insoluble pellet fraction compared to when *HUL5* was intact (Supplementary Fig. 4d, "supernatant" and "pellet" fractions). However, the bulk of RQCsub$_{LONG}$ in all *ltn1*Δ strains remained in the soluble fraction similarly to the soluble protein hexokinase (Supplementary Fig. 4d, "supernatant" and "pellet" fractions). Therefore,

the majority of CATylated RQCsub$_{LONG}$ was soluble whether or not Ltn1-independent degradation was functional.

CAT tails are degrons

We hypothesized that short, mRNA-encoded sequences of alanine and threonine residues are sufficient to confer the same degradation we observed for CATylated proteins. To test this hypothesis, we replaced our model RQC substrates' stalling sequence with three non-stalling arginine residues (preserving the stalling sequence charge) and appended defined alanine and threonine sequences followed by a stop codon (Fig. 4a). These "hard-coded" CAT tails simulated natural CAT tails but had manipulable sequences and were not RQC substrates. If a hard-coded CAT tail suffices for degradation as observed for a naturally CATylated RQC substrate (Fig. 3c), its stability would be higher in *hul5*Δ cells than wild-type. We define this Hul5-dependence as stability$_{hul5\Delta}$ − stability$_{wt}$ (Fig. 4a). While the arginine C-terminus control and alanine/threonine two-mers were not Hul5-dependent, "RRRATA" yielded weak Hul5-dependence (13%) (Fig. 4b). Doubling this motif to form "RRR(ATA)$_2$" increased Hul5 dependence to 80%, but the "RRR(ATA)$_4$" motif (54%) was weaker than "RRR(ATA)$_2$" (Fig. 4b). These results suggest that, similarly to nontemplated CATylation, short hard-coded CAT tails destabilize a model protein in the presence of Hul5. Thus, short CAT tails function as degrons.

We then performed mutagenesis experiments to identify additional CAT tail properties that modulated their degron strength. We assessed the strength of these CAT tail degrons by measuring their Hul5-dependence. After making modifications to "RRRATATA," we found that Hul5-dependence decreased after mutating alanine and threonine to glycine and serine (especially alanine adjacent to arginine), replacing basic residues (common sites of ribosome slowdown[42–44]) adjacent to the CAT tail with non-basic residues, or capping the C-terminus with two leucine residues (a relatively stable C-terminal amino acid[45]) (Fig. 4b,4c). This mutagenesis series suggests that CAT tails are effective degrons when: 1) adjacent to one or more basic amino acids, especially when alanine is directly adjacent, and 2) C-terminal.

We next investigated whether hard-coded CAT tails target proteins for ubiquitylation similarly to natural CAT tails. Stability increased upon bortezomib treatment for "RRRATATA" but not the arginine C-terminus control (Fig. 4d). Pull-down of the strongest CAT tail degron we tested, "RRR(ATA)$_2$", recovered ubiquitin conjugates whose detection was abolished upon *hul5*Δ (Fig. 4e). As for the naturally CATylated RQCsub$_{LONG}$, *hul5*Δ diminished ubiquitin conjugation and did not stabilize a mono-ubiquitylated species (Fig. 4e). Thus, hard-coded CAT tails are sufficient to mark proteins that are not RQC substrates for ubiquitylation. This sufficiency suggests that Ltn1-independent degradation of RQC substrates can occur off the ribosome, unlike Ltn1-dependent degradation[46].

Dissection of CAT tail function

Our work supports the following model: Ltn1 efficiently ubiquitylates substrates that contain lysine in unstructured regions regardless of whether CATylation takes place (Fig. 5a). However, CATylation enhances Ltn1's ability to ubiquitylate structured substrates that lack mobile lysine residues. If Ltn1 fails to ubiquitylate the substrate or is limiting, short (~1kDa)

CAT tails mark that substrate for degradation off the ribosome. To support this model, we sought to test its key predictions and quantify the degree to which CAT tails contribute to Ltn1 function compared to acting as off-ribosome degrons.

Our model predicts that CAT tails are dispensable for degradation of substrates that: 1) are unstructured, and 2) terminate in a non-basic residue (preventing Hul5-dependent degron activity). We constructed such a substrate, $RQCsub_{Rz}$, encoded by an mRNA containing a hammerhead ribozyme that self-cleaves before the stop codon to produce a GFP transcript with a truncated 3' end that stalls ribosomes (Fig. 5b)[47]. Before CATylation, the C-terminal residue of $RQCsub_{Rz}$ is neutrally charged valine and there are too few residues between GFP and the C-terminus to enable formation of the stable GFP conformation[30]. As predicted, neither disruption of CATylation (*rqc2-d98a*) nor loss of Hul5 stabilized $RQCsub_{Rz}$ (Fig. 5b). Thus, unstructured substrates terminating in non-basic amino acids are not CAT tail dependent.

We next revisited $RQCsub_{LONG}$ to dissect how CAT tails mediate its degradation via degron-forming and Ltn1-enhancing activities. We first estimated the contribution of CATylation to Hul5 (required for CAT tail degron activity on this substrate) and Ltn1 by measuring the stabilization caused by *hul5*Δ, assuming that Hul5 and Ltn1 activities are independent (Fig. 5c). Using this analysis, we estimated that Hul5 mediates 40% of CAT tail-dependent degradation and Ltn1 mediates the remaining 60% (Fig. 5d). We were additionally interested in analyzing the size of CAT tails that facilitated Ltn1-mediated degradation. To estimate the contribution of long CAT tails, we co-expressed TEV to cleave $RQCsub_{LONG}$ from the ribosome (and evade Ltn1) if its CAT tails were long enough to expose the buried TEV-cleavage-site (greater than 21 residues) (Fig. 5c). TEV co-expression further dissected Ltn1-mediated degradation into 19% contributed by long CAT tails (TEV-sensitive) and 41% by short CAT tails (TEV-insensitive) (Fig. 5d). To assess the effect of lysine buried in the exit tunnel on CAT tail-mediated degradation, we repeated this analysis after mutating $RQCsub_{LONG}$'s exit tunnel-buried lysine. This mutation eliminated the contribution of short CAT tails to Ltn1 function, but increased the relative contributions of CAT tails to Hul5 and long CAT tails to Ltn1 (Fig. 5d). We conclude that CAT tails facilitate degradation of RQC substrates via Ltn1-dependent (on ribosome) and Ltn1–independent (off-ribosome) pathways. Short CAT tails can enhance Ltn1 function by exposing lysine residues buried in the exit tunnel, as proposed by Kostova et al[25]. Long CAT tails, some of which may emerge from the exit tunnel, can enable Ltn1 to access lysine residues distal from the exit tunnel.

We asked whether the dual functions of CAT tails in degradation of RQC substrates contribute to cellular fitness when RQC is stressed by elevated substrate levels. We increased the influx of endogenous RQC substrates by growing cells in the presence of the translation inhibitor cycloheximide, which increases translational stalling. All *RQC2* and *LTN1* mutant strains grew equally well in the absence of cycloheximide, as assessed by a spot assay (Fig. 5e). While cycloheximide inhibited growth of all the strains we measured, simultaneous disruption of CATylation (*rqc2-d98a*) and Ltn1 resulted in a dramatic synthetic growth defect (Fig. 5e). This synergistic growth defect indicates that CATylation is crucial for cellular fitness in cells with increased stalling when Ltn1 becomes limiting.

Discussion

We propose that CAT tails are bi-functional marks for RQC substrate degradation. On the ribosome, CAT tails enhance Ltn1 activity on structured substrates. Off the ribosome, CAT tails form degrons that mark escaped RQC substrates for degradation when Ltn1 is compromised.

We observed that CAT tails enable Ltn1 to target structured RQC substrates, which are otherwise poor Ltn1 substrates. Structured RQC substrates may arise when translation fails after synthesis of domains competent for co-translational folding; for example, this might occur during non-stop translation when the ribosome synthesizes the entire reading frame but stalls within the poly(A) tail or during abnormally slow translation of inter-domain linkers[44]. The inefficiency of Ltn1 activity on structured RQC substrates is consistent with the mechanism of RING E3 ubiquitin ligases. RING E3s bind to E2 ubiquitin ligases, stabilizing a conformation that primes the E2-ubiquitin bond for ubiquitin transfer[48–50]. For ubiquitin transfer to occur, a nucleophile from the substrate (e.g. the ε-amino group from a lysine residue) attacks the E2-ubiquitin thioester bond[51]. Unstructured regions of an RQC substrate may have enough conformational flexibility for their lysine residues to reach the E2 active site and efficiently acquire ubiquitin. Conversely, lysine residues confined to rigid regions of the RQC substrate may lack the flexibility to move in three-dimensional space and access the E2 active site. We propose that CAT tails act as flexible linkers that allow RQC substrates to sample more three-dimensional space, enabling lysine residues within rigid regions of the substrate to acquire ubiquitin from the E2 active site.

The experiments herein succinctly test the model proposed by Kostova and colleagues regarding the role of CAT tails in degradation of RQC substrates[25]. While this model posits that Ltn1 only ubiquitylates lysine residues immediately proximal to the exit tunnel, our results indicate that Ltn1 can access residues distal to the exit tunnel. *LTN1* perturbation still stabilized substrates lacking residues close (in primary sequence) to the ribosome exit tunnel (Fig. 1f, Supplementary Fig. 1e). Furthermore, addition of lysine residues to the N-terminus of RQC substrates enhanced their degradation, provided the residues appeared in unstructured regions (Fig. 2d–e). In agreement with Kostova and colleagues, we found that short CAT tails can enhance degradation of an RQC substrate by exposing lysine residues buried in the ribosome exit tunnel (Fig. 5d), although this degradation mechanism represented roughly one-fifth of total CAT tail-mediated degradation of a model substrate (Fig. 1f). Ltn1 may efficiently ubiquitylate these newly-exposed residues because polypeptides typically emerge from the ribosome exit tunnel unfolded[52,53]. We propose that RQC substrate tertiary structure, rather than primary structure, determines the efficiency of Ltn1-mediated degradation.

Our work uncovered a second novel function for CATylation: CAT tails form Ltn1-independent degrons. Rather than acting as an inert extension of the RQC substrate, the alanine and threonine residues in CAT tails mark RQC substrates for degradation off the ribosome. Because Ltn1 activity on RQC substrates is restricted to the 60S ribosome[5,46], in the absence of CATylation, cells would be left with a single opportunity to target RQC substrates for degradation. However, by serving as off-ribosome degrons, CAT tails indelibly

mark RQC substrates for degradation throughout their lifetime. The CAT tail degrons we tested depended on Hul5 for ubiquitylation; Hul5 was thus a useful tool to genetically tune CAT tail degron activity. However, we stress that this does not indicate that all CATylated proteins rely on Hul5 for ubiquitylation. Proteasomal degradation of CATylated proteins could involve multiple E3 ubiquitin ligases or could occur though ubiquitin-independent means. Further studies will elucidate the precise degradation mechanism of CAT tail degrons.

Online Methods

Yeast strains, growth conditions, and plasmids

All yeast strains and plasmids used are listed in Supplementary Tables 1 and 2, respectively.Yeast cultures were grown at 30°C (unless otherwise noted) in YPD media or synthetic defined media with appropriate nutrient dropouts.Deletion strains were constructed in the BY4741 background via transformation with PCR products bearing antibiotic selection cassettes (*NATMX6* or *HYGMX6*). These PCR products contained 40bp of homology to the genome on their 5' and 3' ends. Transformants were verified by genomic PCR.

RQC2 mutants were constructed by first replacing 1.5kb 5' and 300bp 3' of the *RQC2* start codon with a *NATMX6* cassette. This gap was repaired in transformants by transformation with a PCR product containing a *LEU2* cassette and *pRQC2-RQC2* variant N-terminus, amplified from plasmids containing these *RQC2* variants. The resultant colonies were verified to have incorporated the desired *RQC2* allele by genomic PCR and sanger sequencing.

Plasmids used in this study were cloned by the Gibson Assembly method[54] using NEBuilder HiFi DNA Assembly Master Mix (New England Biolabs). All plasmids were derived from either the pRS315 or pRS316 vectors. For experiments where multiple exogenous proteins were co-expressed, all of the proteins were expressed from a single plasmid.

TEV treatment

1-liter log-phase yeast cultures at OD600 = 0.6–0.8 were harvested by vacuum filtration and flash frozen in liquid nitrogen. Frozen yeast pellets were lysed by cryo-grinding in a Spex 6750 Freezer Mill for 3 rounds of 10Hz for 2 minutes. The resulting "grindate" was re-solubilized in TEV buffer (25mM HEPES-KOH pH 7.4, 150mM KOAc, 0.5mM EDTA, 10% glycerol, 0.04% Antifoam-B, and EDTA-Free Pierce Protease Inhibitor Mini Tablets; added 1:1 vol:mass) to produce lysate. The lysate was clarified by centrifugation for 5 min at 5000g, then two rounds of 5 min at 10,000g. 1mM DTT was freshly added to the lysate before treatment with 2ul ProTEV Plus enzyme (Promega) per 23ul of lysate at 30°C for 3 hr in a thermocycler. 4x NuPage LDS Sample Buffer (Thermo Fisher Scientific) with 5% β-mercaptoethanol was added at 1:1 vol:vol before boiling at 95°C for 5 min to denature the samples.

Flow cytometry

Log phase yeast growing in synthetic defined media were measured on a BD Accuri C6 flow cytometer (BD Biosciences) with 3–5 biological replicates (independent cultures from separate clones) per condition. Data were analyzed in Matlab; a detailed, step-wise graphic example of this analysis is presented in Supplementary Fig. 6a–d. Plasmid-expressing yeast were selected by gating based on RFP fluorescence. Background signal bleeding from the RFP channel into the GFP channel was calculated using an RFP-only control strain expressing RFP-$(T2A)_2$-GST (Supplementary Fig. 1a) and subtracted before additional calculations. In the case where cultures were treated with bortezomib (LC Laboratories), treatment lasted for 4 hrs.

Statistical analysis

A two-tailed t-test for particular contrast was used to determine whether differences in CAT tail dependence values between substrates were significant. The null hypothesis for the t-test was: $\mu_{rqc2\text{-}d98a + \text{substrate 1}} - \mu_{RQC2\text{-}WT + \text{substrate 1}} = \mu_{rqc2\text{-}d98a + \text{substrate 2}} - \mu_{RQC2\text{-}WT + \text{substrate 2}}$. The linear model was constructed using the raw fluorescence means from each replicate using the “lm” function in R and the linear hypothesis was tested using the “linearHypothesis” function in R.

A one-way ANOVA test (one-tailed) was used to determine whether mean measurements differed between substrates in two different conditions. The null hypothesis was: $\mu_{\text{condition 1}} = \mu_{\text{condition 2}}$.

Immunoprecipitation and immunoblot

In most cases where results were analyzed by immunoblots or immunoprecipitation, a version of the substrate without the expression-normalizing RFP-$(T2A)_2$ module was used. This choice was made to improve clarity by reducing the number of products detected on the gel. The two exceptions to this are Supplementary Fig. 3b and Supplementary Fig. 4d, where an RFP-$(T2A)_2$-containing substrate was shown in an immunoblot.

For whole-cell immunoblots, (0.375/OD600) × ml of log-phase yeast culture between OD600 = 0.4–0.8 were pelleted and resuspended in 15ul 4x NuPage LDS Sample Buffer with 5% β-mercaptoethanol. The sample buffer-resuspended pellets were lysed and denatured by boiling at 95°C for 5 min.

To detect ubiquitin conjugates, cells expressing a plasmid with the bidirectional *pGAL1,10* promoter driving expression of His-Myc-tagged ubiquitin and the construct of interest were used. An additional plasmid that lacked a construct of interest and only contained His-Myc-tagged ubiquitin was used to assess non-specific ubiquitin detection. A 20ml culture of these cells was grown in SD media overnight containing 1% galactose and 2% raffinose to induce expression of tagged ubiquitin and the construct of interest. The culture was pelleted by centrifugation, weighed and resuspended in 100mM Tris pH 7.4, 10 mM EDTA at 500ul: 25mg pellet. The resuspended culture was added dropwise into liquid nitrogen and cryo-ground as described above. The resultant grindate was resolubilized 1:1 mass:vol in buffer to produce lysate that had a final composition of 50mM Tris pH 7.4, 5mM EDTA, 20mM N-

ethylmaleimide (added from a fresh 2M stock in ethanol; irreversibly inhibits deubiquitinases), 0.5% NP-40, 0.04% Antifoam-B, and EDTA-Free Pierce Protease Inhibitor Mini Tablets. The lysate was clarified by centrifugation at 5000g for 5 min and twice at 10,000g for 5 min. The clarified lysate incubated with buffer-equilibrated GFP-Trap magnetic agarose resin (Chromotek) (15ul slurry:25mg pellet) for 1 hr 4°C with rotation, washed 5 times in buffer, and eluted by boiling in 20ul 2x NuPage LDS Sample Buffer with 5% β-mercaptoethanol per 15ul resin for 95°C for 5 min.

For SDS-PAGE, all samples were run on Novex Nupage 4–12% Bis-Tris gels (Thermo Fisher Scientific) and transferred onto 0.45um nitrocellulose membranes (Bio-Rad) using a Transblot Turbo (Bio-Rad). For ubiquitin detection, the membrane was cut at the 50kDa marker to separate unmodified bands from potential poly-ubiquitylated conjugates; these two halves of the membrane were stained separately to enhance detection of the ubiquitin conjugates. Membranes were blocked for 1 hr with 5% milk in TBST at room temperature before staining with antibodies, either overnight at 4°C or for 4 hr at room temperature. Membranes were stained with the following primary antibodies: 1:2000 Pierce mouse anti-GFP (Thermo Fisher Scientific), 1:1000 rabbit anti-GFP (Life Technologies), 1:3000 rabbit anti-Hexokinase (US Biological), 1:1000 Pierce mouse anti-6xHis (Thermo Fisher Scientific), 1:1000 Pierce mouse anti-Myc (Thermo Fisher Scientific). The following secondary antibodies were used to stain membranes at 1:5000: IRDye 800CW donkey anti-mouse, IRDye 800CW goat anti-rabbit, IRDye 680RD goat anti-rabbit, or IRDye 680RD goat anti-mouse (LiCor Biosciences). A LiCor Odyssey (LiCor Biosciences) was used to scan immunoblots.

Amino acid analysis

Yeast lysates were produced as in the “TEV treatment” section, except the following buffer was used to resolubilize the grindate: 50mm HEPES pH7.4, 100mM NaCl, 0.5 mM EDTA. 400ul of clarified lysate was immunoprecipitated 20ul magnetic agarose GFP trap resin. After six washes, the resin was eluted by pipetting up and down in 40ul of buffer adjusted to pH 2.5. Eluates were subjected to amino acid analysis at the UC Davis Genome Center as described in Shen et al[19].

Supernatant-pellet fractionation

The protocol for supernatant-pellet fractionation of yeast lysates was derived from Wallace et al[55]. Yeast grindate were produced as described in the “TEV treatment” section. Soluble Protein Buffer (20mM HEPES-KOH pH 7.4, 120mM KCl, 2mM EDTA, 0.2mM DTT, 0.04% Antifoam-B, EDTA-Free Pierce Protease Inhibitor Mini Tablets; added 4:1 vol:mass) was used to resolubilize the grindate at 4°C. The resolubilized grindate was centrifuged at 4°C for 1 min at 3000g for clarification. This clarified lysate was used as the “input” fraction, 20ul of which was mixed with 20ul of 4x NuPage LDS Sample Buffer with 5% β-mercaptoethanol and denatured by boiling at 95°C for 5 min. 300ul of clarified lysate was spun at 100,000g for 20 min in a TLA-110 rotor (Beckman Coulter) at 4°C. The “supernatant” fraction was denatured as described for the input fraction. The pellet was washed with 500ul of Soluble Protein Buffer and vortexed for 2 min, then centrifuged again at 100,000g for 20 min at 4°C. The supernatant was thoroughly removed from the tube and

250ul of room temperature Insoluble Protein Buffer (20mM HEPES-KOH pH 7.4, 150mM NaCl, 2mM EDTA, 2%SDS, 2mM DTT, 0.04% Antifoam-B, 8M urea, EDTA-Free Pierce Protease Inhibitor Mini Tablets) was added to the pellet. The pellet was resuspended by dislodging with a pipette tip and vortexing for 25 min until the solution was clear. The resuspended pellet was centrifuged at 19,000g for 5 min at room temperature, and the supernatant was collected. This supernatant was defined as the “pellet” fraction, and was denatured as described above for the input fraction. 5ul of the denatured fractions were run on SDS-PAGE.

Yeast spot assay

Late log phase yeast grown in YPD were diluted to OD600 = 0.4 and 200ul of culture was placed in a sterile 96-well plate (Greiner Bio-one). 4 1:10 serial dilutions of the cultures into YPD were made in the plate. 10ul of yeast culture from the wells were transferred to YPD agar plates without drugs or YPD agar plates with 50ng/ml or 100ng/ml cycloheximide (Sigma-Aldrich). After drying, the plates were incubated at 30°C. The drug-free and 50ng/ml cycloheximide plates were imaged after two days of growth. The 100ng/ml cycloheximide plate was imaged after two weeks of growth.

Supplementary Material

Refer to Web version on PubMed Central for supplementary material.

Acknowledgements

We thank S. Marqusee, J. Frydman, R. Hegde, and B. Lu for helpful discussions. We thank L. Steinman, R. Kopito, E.P. Geiduschek, and the members of the Brandman and Kopito Labs for comments on the manuscript. We acknowledge J. Work (Stanford University, Stanford, CA, USA) for his gift of the “10–31” degron and control plasmids. John Schulze (University of California at Davis, Davis, CA, USA) performed the Amino Acid Analysis at the UC Davis Genome Center Molecular Structure Facility. Stanford University (O.B.), the US National Institutes of Health (R01GM115968 to O.B.), and the National Institute of General Medical Sciences of the US National Institutes of Health (T32GM007276 to C.S.S.) supported this work.

References

1. Bengtson MH & Joazeiro CAP Role of a ribosome-associated E3 ubiquitin ligase in protein quality control. Nature 467, 470–473 (2010). [PubMed: 20835226]
2. Brandman O et al. A ribosome-bound quality control complex triggers degradation of nascent peptides and signals translation stress. Cell 151, 1042–1054 (2012). [PubMed: 23178123]
3. Defenouillère Q et al. Cdc48-associated complex bound to 60S particles is required for the clearance of aberrant translation products. Proc. Natl. Acad. Sci. U. S. A 110, 5046–5051 (2013). [PubMed: 23479637]
4. Tsuboi T et al. Dom34:hbs1 plays a general role in quality-control systems by dissociation of a stalled ribosome at the 3’ end of aberrant mRNA. Mol. Cell 46, 518–529 (2012). [PubMed: 22503425]
5. Shao S, von der Malsburg K & Hegde RS Listerin-dependent nascent protein ubiquitination relies on ribosome subunit dissociation. Mol. Cell 50, 637–648 (2013). [PubMed: 23685075]
6. Letzring DP, Dean KM & Grayhack EJ Control of translation efficiency in yeast by codon–anticodon interactions. RNA (2010). doi:10.1261/rna.2411710
7. Ito-Harashima S, Kuroha K, Tatematsu T & Inada T Translation of the poly (A) tail plays crucial roles in nonstop mRNA surveillance via translation repression and protein destabilization by proteasome in yeast. Genes Dev. 21, 519–524 (2007). [PubMed: 17344413]

8. Simms CL, Yan LL & Zaher HS Ribosome Collision Is Critical for Quality Control during No-Go Decay. Mol. Cell 68, 361–373.e5 (2017). [PubMed: 28943311]
9. Juszkiewicz S et al. ZNF598 Is a Quality Control Sensor of Collided Ribosomes. Mol. Cell 72, 469–481.e7 (2018). [PubMed: 30293783]
10. Ikeuchi K et al. Collided ribosomes form a unique structural interface to induce Hel2-driven quality control pathways. EMBO J. e100276 (2019). [PubMed: 30609991]
11. Sundaramoorthy E et al. ZNF598 and RACK1 Regulate Mammalian Ribosome-Associated Quality Control Function by Mediating Regulatory 40S Ribosomal Ubiquitylation. Mol. Cell 65, 751–760.e4 (2017). [PubMed: 28132843]
12. Juszkiewicz S & Hegde RS Initiation of Quality Control during Poly(A) Translation Requires Site-Specific Ribosome Ubiquitination. Mol. Cell 65, 743–750.e4 (2017). [PubMed: 28065601]
13. Matsuo Y et al. Ubiquitination of stalled ribosome triggers ribosome-associated quality control. Nat. Commun 8, 159 (2017). [PubMed: 28757607]
14. Shoemaker CJ, Eyler DE & Green R Dom34:Hbs1 promotes subunit dissociation and peptidyl-tRNA drop-off to initiate no-go decay. Science 330, 369–372 (2010). [PubMed: 20947765]
15. Pisareva VP, Skabkin MA, Hellen CUT, Pestova TV & Pisarev AV Dissociation by Pelota, Hbs1 and ABCE1 of mammalian vacant 80S ribosomes and stalled elongation complexes. EMBO J. 30, 1804–1817 (2011). [PubMed: 21448132]
16. Lyumkis D et al. Structural basis for translational surveillance by the large ribosomal subunit-associated protein quality control complex. Proceedings of the National Academy of Sciences 111, 15981–15986 (2014).
17. Sitron CS, Park JH & Brandman O Asc1, Hel2, and Slh1 couple translation arrest to nascent chain degradation. RNA 23, 798–810 (2017). [PubMed: 28223409]
18. Shao S, Brown A, Santhanam B & Hegde RS Structure and assembly pathway of the ribosome quality control complex. Mol. Cell 57, 433–444 (2015). [PubMed: 25578875]
19. Shen PS et al. Protein synthesis. Rqc2p and 60S ribosomal subunits mediate mRNA-independent elongation of nascent chains. Science 347, 75–78 (2015). [PubMed: 25554787]
20. Osuna BA, Howard CJ, Kc S, Frost A & Weinberg DE In vitro analysis of RQC activities provides insights into the mechanism and function of CAT tailing. Elife 6, (2017).
21. Choe Y-J et al. Failure of RQC machinery causes protein aggregation and proteotoxic stress. Nature 531, 191–195 (2016). [PubMed: 26934223]
22. Yonashiro R et al. The Rqc2/Tae2 subunit of the ribosome-associated quality control (RQC) complex marks ribosome-stalled nascent polypeptide chains for aggregation. Elife 5, e11794 (2016). [PubMed: 26943317]
23. Defenouillère Q et al. Rqc1 and Ltn1 prevent CAT-tail induced protein aggregation by efficient recruitment of Cdc48 on stalled 60S subunits. J. Biol. Chem jbc–M116 (2016). [PubMed: 27129277]
24. Chu J et al. A mouse forward genetics screen identifies LISTERIN as an E3 ubiquitin ligase involved in neurodegeneration. Proc. Natl. Acad. Sci. U. S. A 106, 2097–2103 (2009). [PubMed: 19196968]
25. Kostova KK et al. CAT-tailing as a fail-safe mechanism for efficient degradation of stalled nascent polypeptides. Science 357, 414–417 (2017). [PubMed: 28751611]
26. Dimitrova LN, Kuroha K, Tatematsu T & Inada T Nascent peptide-dependent translation arrest leads to Not4p-mediated protein degradation by the proteasome. J. Biol. Chem 284, 10343–10352 (2009). [PubMed: 19204001]
27. Donnelly MLL et al. Analysis of the aphthovirus 2A/2B polyprotein ‘cleavage’mechanism indicates not a proteolytic reaction, but a novel translational effect: a putative ribosomal ‘skip’. J. Gen. Virol 82, 1013–1025 (2001). [PubMed: 11297676]
28. Szymczak AL & Vignali DA A. Development of 2A peptide-based strategies in the design of multicistronic vectors. Expert Opin. Biol. Ther 5, 627–638 (2005). [PubMed: 15934839]
29. Voss NR, Gerstein M, Steitz TA & Moore PB The geometry of the ribosomal polypeptide exit tunnel. J. Mol. Biol 360, 893–906 (2006). [PubMed: 16784753]

30. Kelkar DA, Khushoo A, Yang Z & Skach WR Kinetic analysis of ribosome-bound fluorescent proteins reveals an early, stable, cotranslational folding intermediate. J. Biol. Chem 287, 2568–2578 (2012). [PubMed: 22128180]

31. Patterson GH, Knobel SM, Sharif WD, Kain SR & Piston DW Use of the green fluorescent protein and its mutants in quantitative fluorescence microscopy. Biophys. J 73, 2782–2790 (1997). [PubMed: 9370472]

32. Pédelacq J-D, Cabantous S, Tran T, Terwilliger TC & Waldo GS Engineering and characterization of a superfolder green fluorescent protein. Nat. Biotechnol 24, 79–88 (2006). [PubMed: 16369541]

33. Batey S & Clarke J Apparent cooperativity in the folding of multidomain proteins depends on the relative rates of folding of the constituent domains. Proc. Natl. Acad. Sci. U. S. A 103, 18113–18118 (2006). [PubMed: 17108086]

34. Nilsson OB et al. Cotranslational folding of spectrin domains via partially structured states. Nat. Struct. Mol. Biol 24, 221–225 (2017). [PubMed: 28112730]

35. Kamiyama D et al. Versatile protein tagging in cells with split fluorescent protein. Nat. Commun 7, 11046 (2016). [PubMed: 26988139]

36. Crosas B et al. Ubiquitin chains are remodeled at the proteasome by opposing ubiquitin ligase and deubiquitinating activities. Cell 127, 1401–1413 (2006). [PubMed: 17190603]

37. Maurer MJ et al. Degradation Signals for Ubiquitin-Proteasome Dependent Cytosolic Protein Quality Control (CytoQC) in Yeast. G3 6, 1853–1866 (2016). [PubMed: 27172186]

38. Koegl M et al. A novel ubiquitination factor, E4, is involved in multiubiquitin chain assembly. Cell 96, 635–644 (1999). [PubMed: 10089879]

39. Aviram S & Kornitzer D The ubiquitin ligase Hul5 promotes proteasomal processivity. Mol. Cell. Biol 30, 985–994 (2010). [PubMed: 20008553]

40. Fang NN, Ng AHM, Measday V & Mayor T Hul5 HECT ubiquitin ligase plays a major role in the ubiquitylation and turnover of cytosolic misfolded proteins. Nat. Cell Biol 13, 1344–1352 (2011). [PubMed: 21983566]

41. Fang NN & Mayor T Hul5 ubiquitin ligase: good riddance to bad proteins. Prion 6, 240–244 (2012). [PubMed: 22561164]

42. Charneski CA & Hurst LD Positively charged residues are the major determinants of ribosomal velocity. PLoS Biol. 11, e1001508 (2013). [PubMed: 23554576]

43. Requião RD, de Souza HJA, Rossetto S, Domitrovic T & Palhano FL Increased ribosome density associated to positively charged residues is evident in ribosome profiling experiments performed in the absence of translation inhibitors. RNA Biol. 13, 561–568 (2016). [PubMed: 27064519]

44. Weinberg DE et al. Improved Ribosome-Footprint and mRNA Measurements Provide Insights into Dynamics and Regulation of Yeast Translation. Cell Rep. 14, 1787–1799 (2016). [PubMed: 26876183]

45. Koren I et al. The Eukaryotic Proteome Is Shaped by E3 Ubiquitin Ligases Targeting C-Terminal Degrons. Cell 173, 1622–1635.e14 (2018). [PubMed: 29779948]

46. Doamekpor SK et al. Structure and function of the yeast listerin (Ltn1) conserved N-terminal domain in binding to stalled 60S ribosomal subunits. Proc. Natl. Acad. Sci. U. S. A 113, E4151–60 (2016). [PubMed: 27385828]

47. Meaux S & Van Hoof A Yeast transcripts cleaved by an internal ribozyme provide new insight into the role of the cap and poly(A) tail in translation and mRNA decay. RNA 12, 1323–1337 (2006). [PubMed: 16714281]

48. Ozkan E, Yu H & Deisenhofer J Mechanistic insight into the allosteric activation of a ubiquitin-conjugating enzyme by RING-type ubiquitin ligases. Proc. Natl. Acad. Sci. U. S. A 102, 18890–18895 (2005). [PubMed: 16365295]

49. Plechanovová A, Jaffray EG, Tatham MH, Naismith JH & Hay RT Structure of a RING E3 ligase and ubiquitin-loaded E2 primed for catalysis. Nature 489, 115–120 (2012). [PubMed: 22842904]

50. Pruneda JN et al. Structure of an E3: E2 Ub complex reveals an allosteric mechanism shared among RING/U-box ligases. Mol. Cell 47, 933–942 (2012). [PubMed: 22885007]

51. Deshaies RJ & Joazeiro CAP RING Domain E3 Ubiquitin Ligases. Annual Review of Biochemistry 78, 399–434 (2009).

52. Cabrita LD, Hsu S-TD, Launay H, Dobson CM & Christodoulou J Probing ribosome-nascent chain complexes produced in vivo by NMR spectroscopy. Proc. Natl. Acad. Sci. U. S. A 106, 22239–22244 (2009). [PubMed: 20018739]

53. Eichmann C, Preissler S, Riek R & Deuerling E Cotranslational structure acquisition of nascent polypeptides monitored by NMR spectroscopy. Proc. Natl. Acad. Sci. U. S. A 107, 9111–9116 (2010). [PubMed: 20439768]

54. Gibson DG et al. Enzymatic assembly of DNA molecules up to several hundred kilobases. Nat. Methods 6, 343–345 (2009). [PubMed: 19363495]

55. Wallace EWJ et al. Reversible, Specific, Active Aggregates of Endogenous Proteins Assemble upon Heat Stress. Cell 162, 1286–1298 (2015). [PubMed: 26359986]

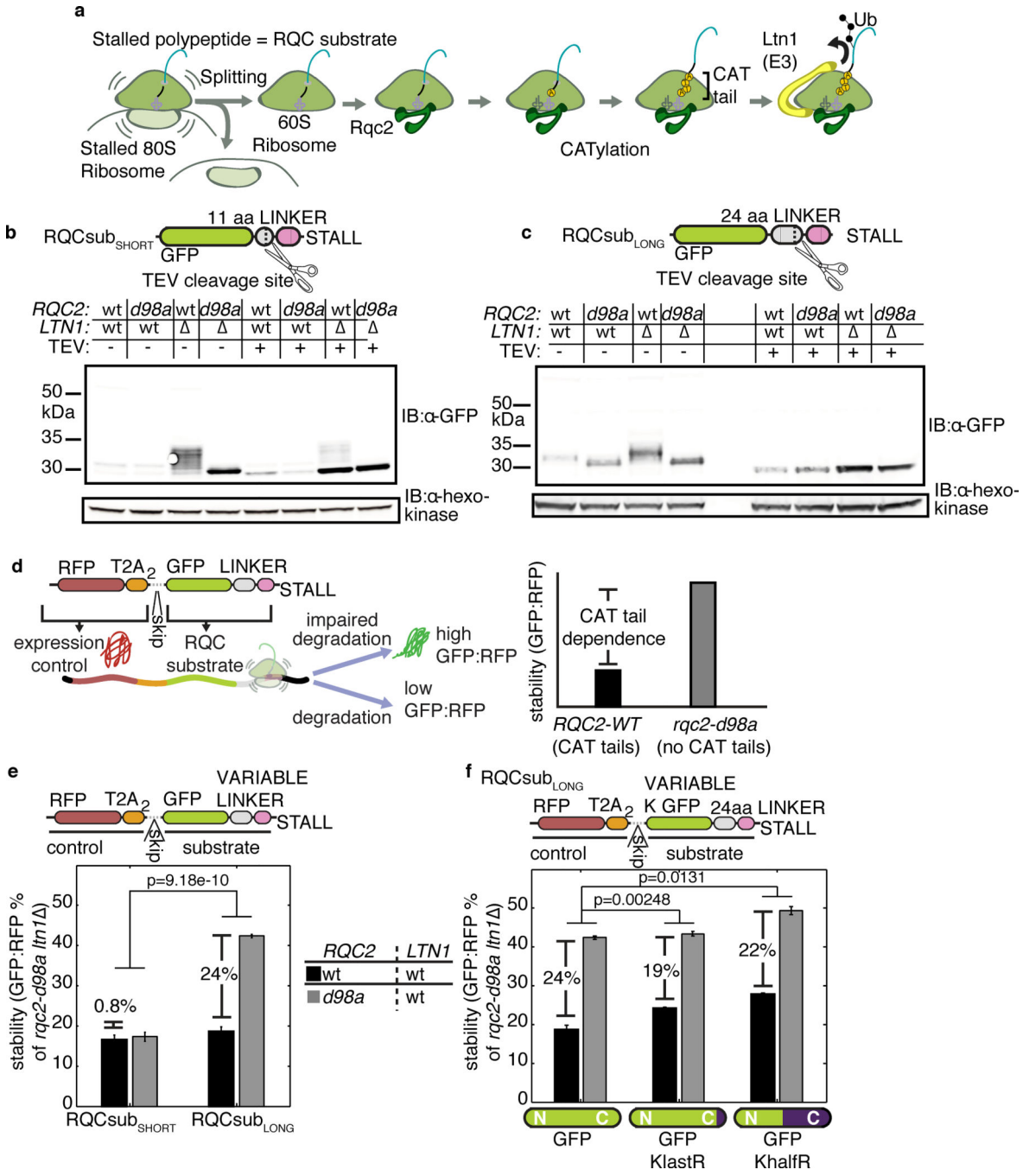

Figure 1 |. Loss of CAT tails stabilizes specific RQC substrates.

a, Model of the RQC pathway. Stalled ribosomes are recognized by a set of factors that facilitate separation of the ribosomal subunits. Rqc2 binds the 60S ribosome-stalled polypeptide complex and directs extension of the stalled polypeptide (RQC substrate) with a CAT tail. Ltn1 binds and ubiquitylates the stalled polypeptide. **b & c,** immunoblots (IBs) of lysates containing two model RQC substrates (schematics above) with and without tobacco etch virus (TEV) protease treatment. GFP, green fluorescent protein. **d,** Schematic of expression-controlled model RQC substrate and definitions of “stability” and “CAT-tail

dependence." RFP, red fluorescent protein. **e & f,** Stability measurements from expression-controlled model RQC substrates with different linker lengths and mutated lysines (0,1, or 10 C-terminal lysines mutated to arginine in GFP). Stability data are reported as means, normalized to the value from the *rqc2-d98a ltn1*Δ strain. CAT tail dependence is indicated with a percent value. Error bars indicate s.e.m. from n = 5 independent cultures and p-values from indicated comparisons of CAT tail dependence are indicated above (16 degrees of freedom, d.o.f.). P-values are derived from a two-tailed t-test for particular contrast.

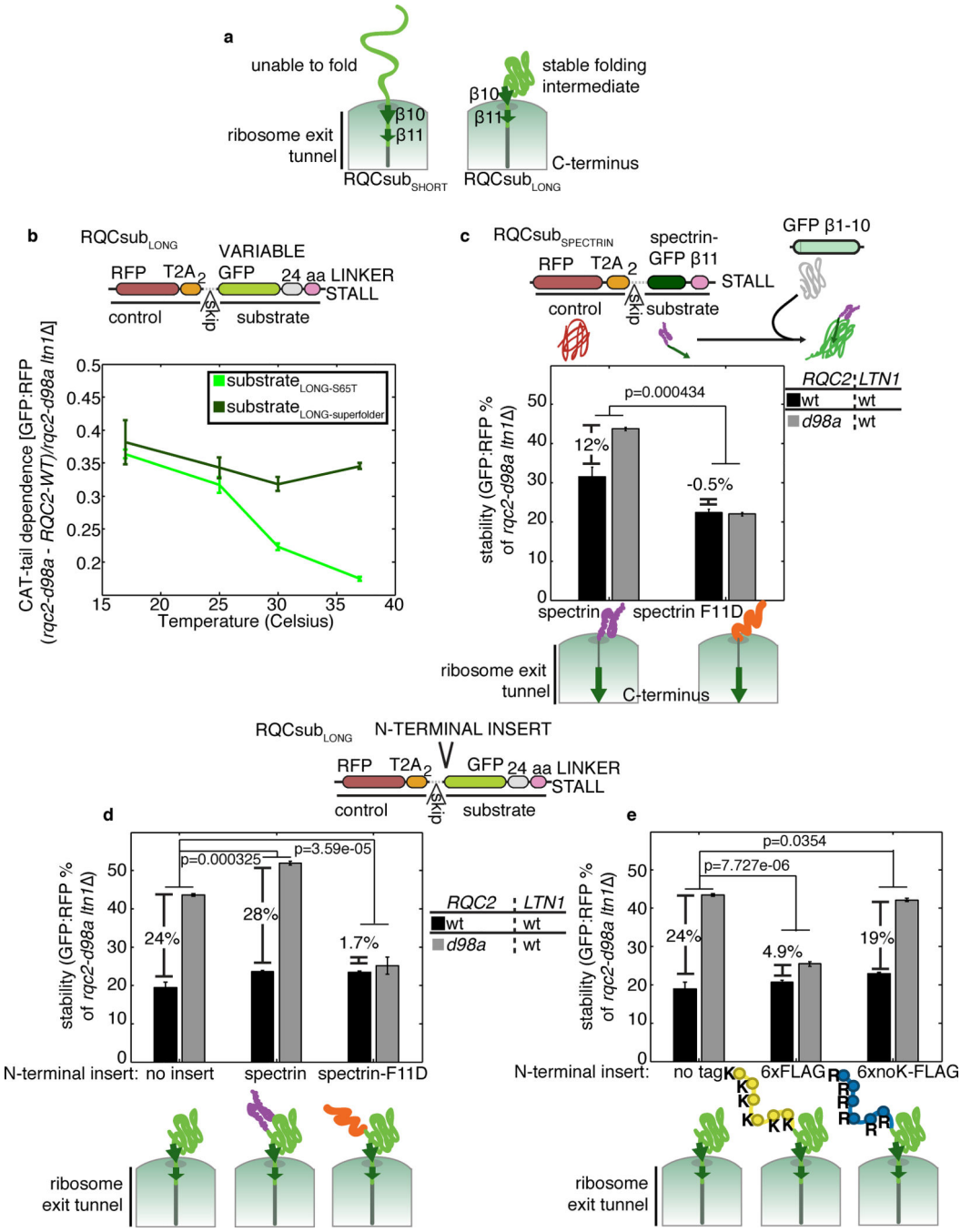

Figure 2 |. Conditions that favor RQC substrate folding increase CAT tail dependence.

a, Cartoon of folding states for $RQCsub_{SHORT}$ and $RQCsub_{LONG}$, emerging from the ribosome exit tunnel. **b,** CAT tail dependence measurements at different incubation temperatures for $RQCsub_{LONG}$ with two different GFP variants (S65T and superfolder). **c,** Normalized stability and CAT tail dependence for a model RQC substrate that can be measured using a split GFP, which features a spectrin R16 domain with or without a fold-disrupting F11D mutation. **d-e,** Normalized stability and CAT tail dependence of variants of $RQCsub_{LONG}$ with added N-terminal domains (folded or unfolded spectrin variants and

6xFLAG and 6xnoK-FLAG) appended to GFP. For all plots, data is normalized as in Fig. 1f and error bars indicate s.e.m. from n = 3 independent cultures. P-values from two-tailed t-tests for particular contrast are displayed above the bars (8 d.o.f.).

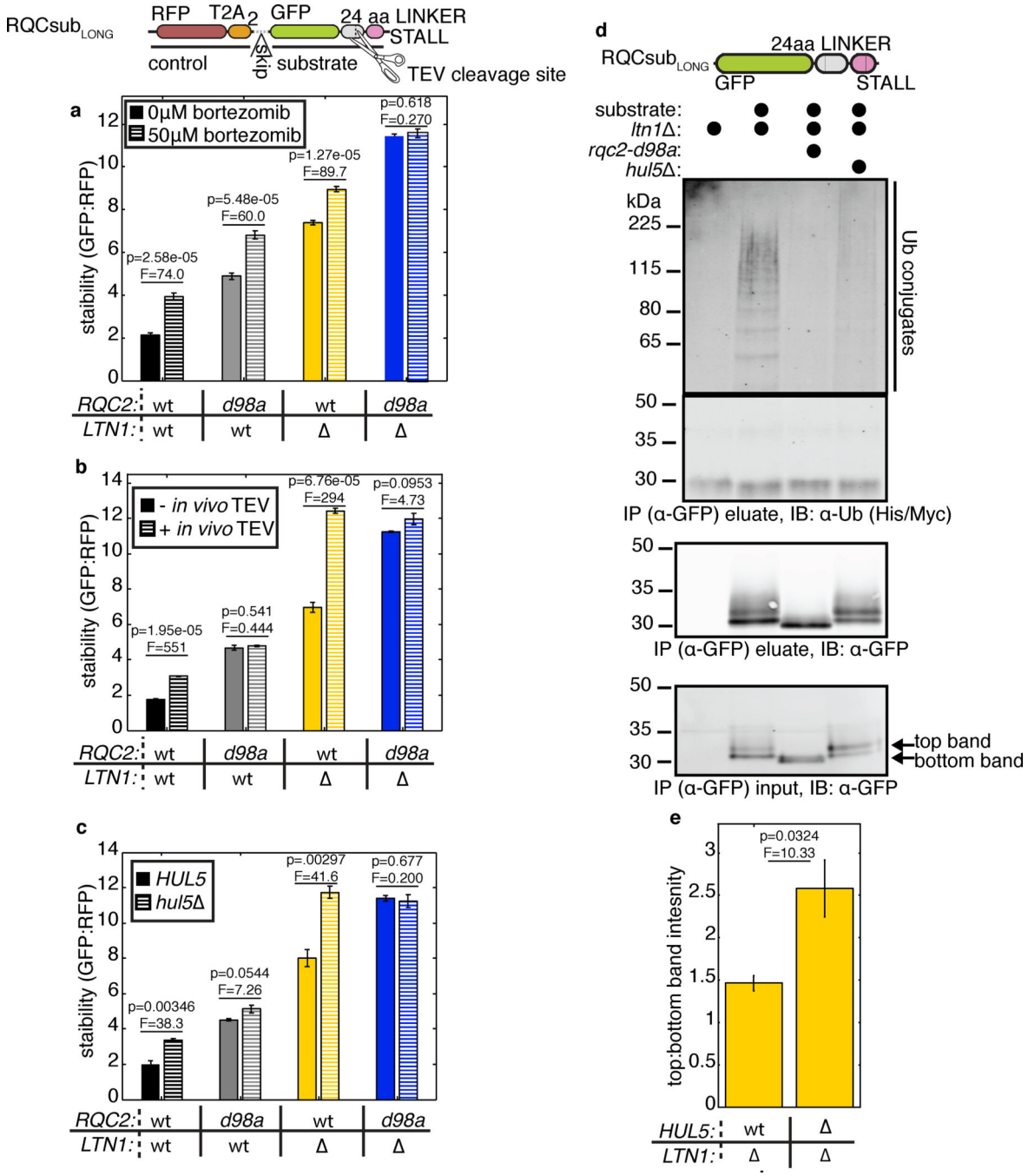

Figure 3 |. CATylated RQC substrates are degraded independently of Ltn1.

a-c, Mean stability of $RQCsub_{LONG}$ in indicated strains after perturbation with the proteasome inhibitor bortezomib, TEV protease co-expression, or *HUL5* deletion (details in panel legend; results from one-tailed, one-way ANOVA tests with 4 d.o.f. indicated above bars). **d,** Analysis of $RQCsub_{LONG}$ and associated ubiquitin by immunoprecipitation (IP) from indicated cell lysates and IB. **e,** Densitometry analysis of two bands seen in $RQCsub_{LONG}$ IBs from whole cell extract, with results from a one-way ANOVA test (one-

tailed, 4 d.o.f.) shown above the bars. Raw images are shown in Supplementary Fig. 4a. For all plots, error bars represent s.e.m. from n = 3 independent cultures.

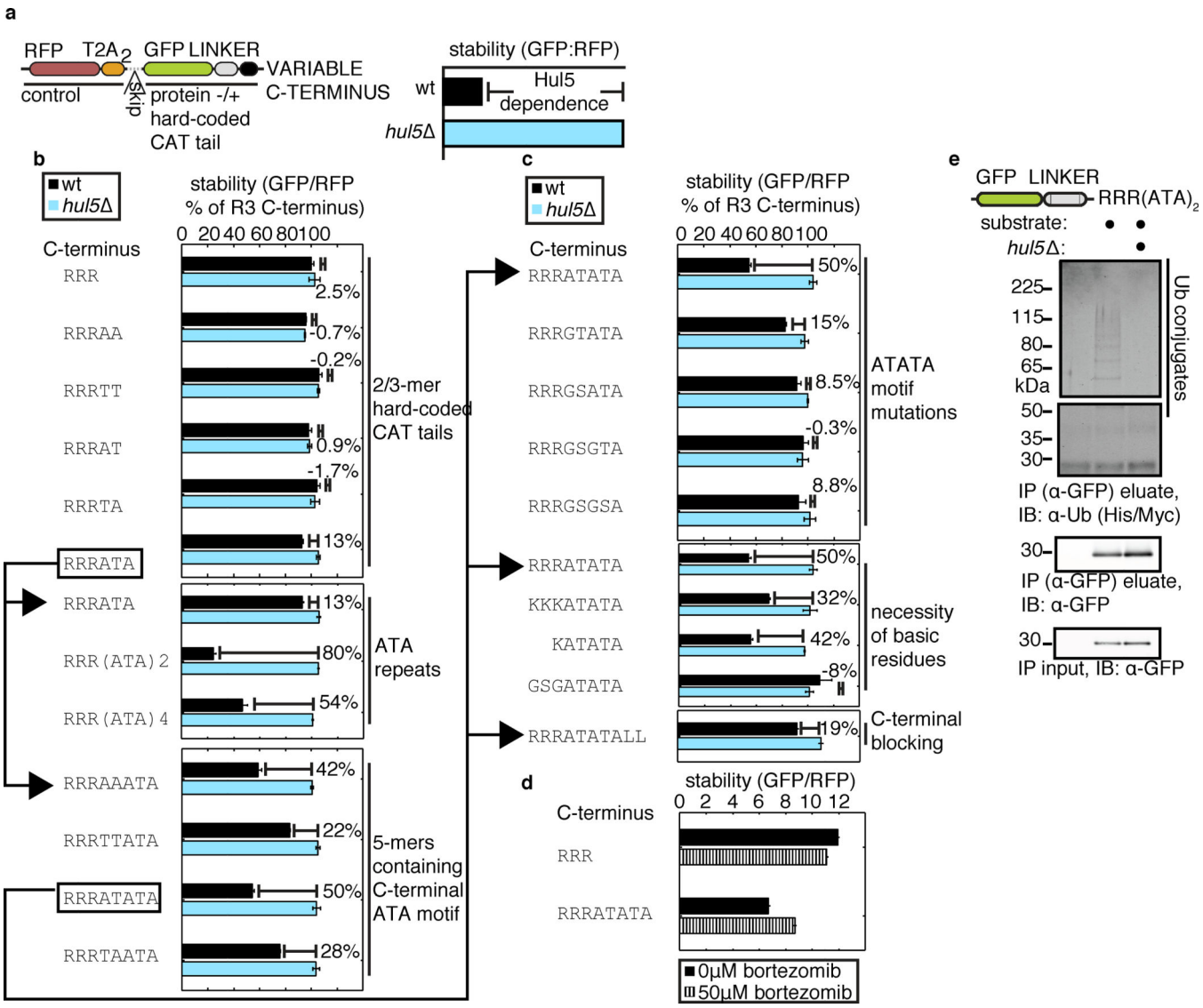

Figure 4 |. CAT tails are degrons.

a, Schematic of the hard-coded CAT tail construct scaffold, terminating in “RRR” encoded by non-stalling codons, and definition of Hul5 dependence which is used as a measure for CAT tail degron strength. **b-c,** Normalized stability measurements of hard-coded CAT tail constructs with indicated C-termini in wild-type and *hul5*Δ cells. Data are presented as mean, normalized to the “RRR” alone construct in wild-type. **d,** Mean stability measurements from wild-type yeast expressing the indicated hard-coded CAT tails, treated with bortezomib. **e,** Analysis of “$(ATA)_2$” hard-coded CAT tail construct by IB after IP from lysate. For all plots, error bars represent s.e.m. from n = 3 independent cultures.

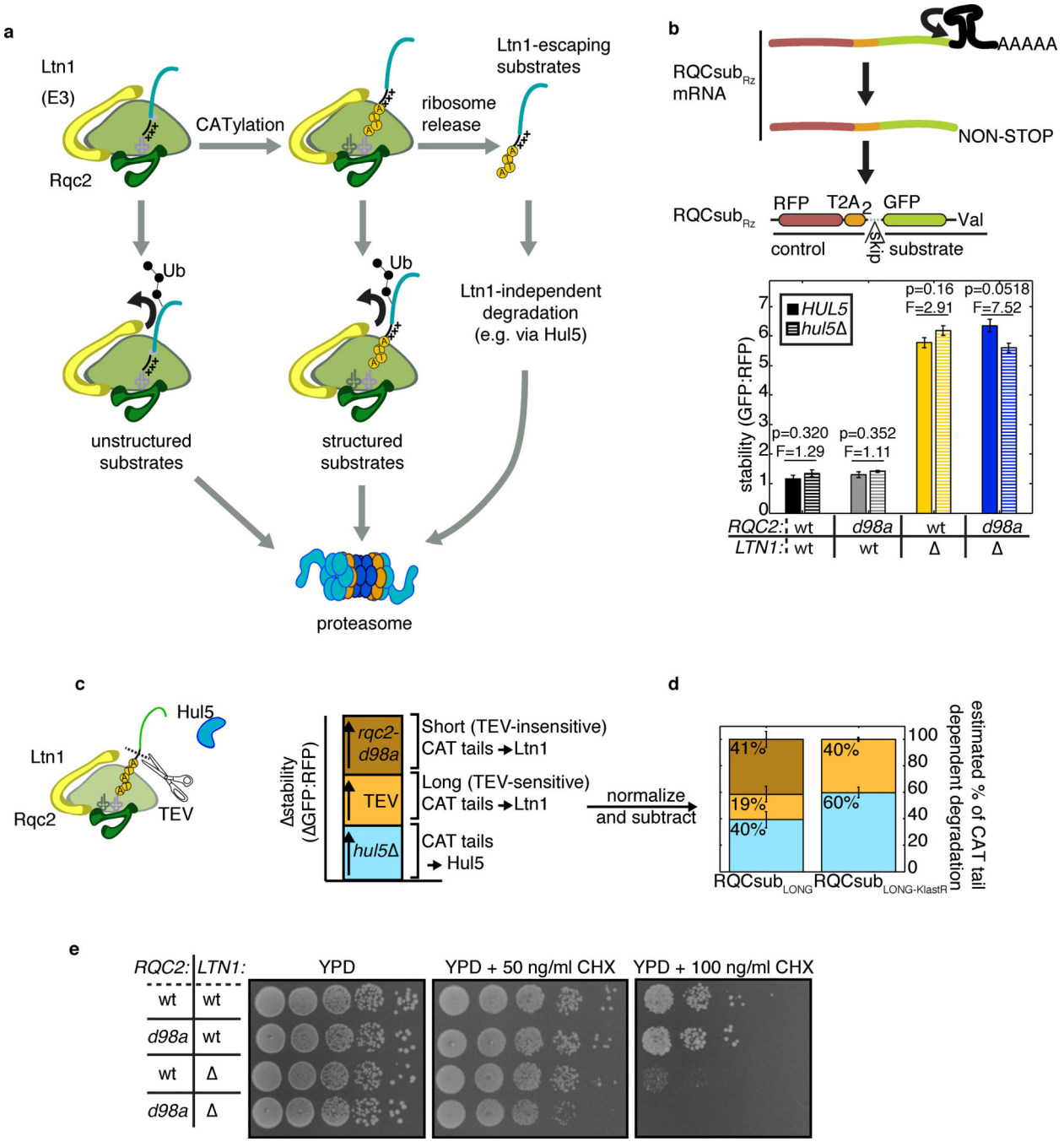

Figure 5 |. Decomposition of the contribution of CAT tails to RQC substrate degradation.

a, Model for how CAT tails enable degradation of RQC substrates by Ltn1-enhancing and degron-forming activities. For unstructured substrates, ubiquitylation by Ltn1 occurs efficiently without CAT tails. CAT tails facilitate ubiquitylation of structured substrates. If Ltn1 fails, substrates released from the ribosome can be targeted for degradation, which depended on Hul5 for the substrates we measured. **b,** Mean stability of RQCsub$_{Rz}$ substrate whose mRNA self-cleaves and leaves thus stalls ribosomes without a polybasic tract (see schematic above). Error bars indicate s.e.m. from n = 3 independent cultures. **c,** Scheme to

decompose the contribution of CAT tails to Ltn1 and Hul5 (degron) function through combined perturbations to delete *HUL5*, remove long CAT tails with *in vivo* TEV cleavage, then mutate *RQC2*. **d,** Estimation of the contribution of Ltn1 (on-ribosome) and Hul5 (required for off-ribosome degron function) to CAT tail-mediated degradation of $RQCsub_{LONG}$ and $RQCsub_{LONG}$ with the C-terminal GFP lysine residue mutated ($RQCsub_{LONG\text{-}KlastR}$, as in Fig. 1f). Data are presented as mean, and error bars indicate s.e.m. from n = 3 independent cultures. Raw data are presented in Supplementary Fig. 5a. e, Spot assay for indicated strains grown with or without the translation inhibitor cycloheximide (CHX).